ISSN: 2716-9227 Algerian Journal of Engineering and Technology 04 (2021) 066–073 e-ISSN: 2716-9278

Algerian Journal of Engineering and Technology

Journal homepage: https://jetjournal.org/index.php/ajet

Original Article

DFT and molecular dynamic simulation study on the corrosion inhibition of Aluminum by some flavonoids of *Guiera Senegalensis* leaves

Ayuba Abdullahi[a]* and Abubakar Muhammad[b]

[a] *Department of Pure and Industrial Chemistry, Faculty of Physical Sciences, Bayero University, Kano, Nigeria.*
[b]*Department of Science and Technology Education, Faculty of Education, Bayero University, Kano, Nigeria.*

ARTICLE INFO

Article history:
Received 28 October 2020
Revised 17 March 2021
Accepted 18 March 2021

Keywords:
Corrosion inhibition;
Guiera senegalensis;
Flavonoids;
DFT.

ABSTRACT

Quantum chemical calculations and molecular dynamics simulations were performed to investigate the effect of four flavonoids compounds (Kaempferol, Quercetin, Myricetin and Rhamnetin) from *Guiera Senegalensis* leaves on corrosion inhibition of aluminium metal in vapour phase. Quantum chemical parameters including E_{HOMO}, E_{LUMO}, energy gap (ΔE), electronegativity (χ), global hardness (η), global softness (σ) and fraction of electrons transferred (ΔN) from the flavonoid molecule to the aluminium surface were calculated and the results indicate that the larger the molecular size the better the inhibition efficiency. Local reactive sites through Fukui indices were also calculated to explain the effect of electronic and structural features of the flavonoid compounds present in the leaves extract of *Guiera senegalensis* (GS). The results showed that the point of interaction of inhibitor molecule with the Al(1 1 0) surface were through hydroxyl and carbonyl functional groups of the studied compounds. Molecular dynamic simulations revealed that the adsorption behaviour of each flavonoid molecule on Al(1 1 0) surface through quench dynamics were found to obey the mechanism of physical adsorption and the more negative is the adsorption energy between the inhibitor-metal surface the better inhibition performance of the molecule on Al(1 1 0) surface.

1. Introduction

Corrosion is a natural phenomenon which can be regarded either chemical or electrochemical in nature [1]. Usually, metal gets oxidized in the presence of acids, alkali, salts and sulphides. Acids such as hydrofluoric acid, hydrochloric acid, nitric acid and phosphoric acid are used in the industries for pickling, etching and descaling of metals [2-4]. These are processes that generally lead to substantial loss of the metal to corrosion. Owing to its corrosion resistance, lightweight, high strength, recyclability, formability, durability, ductility, and conductivity, Aluminium is an exceptionally valuable metal. The metal and its alloys find extensive and large number of applications in various industries in different capacities [5] such as chemical, oil and gas transportation, automobiles, construction among others. The corrosion protection of Aluminium and its alloys are the subject of tremendous technological importance worldwide due to the increased industrial applications of these materials [6]. Among the alternative ways of protecting metals from corrosion, organic compounds containing polar functional groups of the heteroatoms nitrogen, oxygen or sulphur atoms in a conjugated system have been identified to exhibit good inhibiting properties [7]. The inhibition occurs via adsorption of these molecules on the surface of the corroding metal and the performance of the inhibitor depends on the mechanical, structural and chemical

* *Corresponding author. Tel.: +2348062771500*
E-mail address: *ayubaabdullahi@buk.edu.ng*
Peer review under responsibility of University of Echahid Hamma Lakhdar.

http://dx.doi.org/10.5281/zenodo.4636546

characteristics of the adsorption layers of the metal under particular conditions [8].

Experimental procedures are very useful ways to explain the inhibition mechanism between the metal and inhibitor molecules but they are often expensive and consume a lot of time. Continuing advancement in hardware and software tools has opened the door for powerful use of computational chemistry in corrosion inhibition studies. Numerous quantum chemical methods and molecular modelling techniques have been implemented to correlate the inhibition performance of the inhibitors with their molecular properties [5]. Quantum chemical calculations have been broadly used to understand the reaction mechanism; they have also been confirmed to be a powerful computational research tool for investigating the corrosion inhibition of metals [9]. It has been proved that the efficiency of inhibitor molecule is related to its electronic and spatial molecular structure, relating the quantum chemical parameters and inhibition efficiency [10]. Quantum chemical methods and molecular modelling techniques allow the description of a large number of molecular quantities illustrating the reactivity, binding properties and shape of a complete inhibitor molecule as well as molecular fragments and substituents attached to it. Theoretical parameters offer two major advantages: the molecules, their various substituents and fragments can be characterized directly on the basis of their molecular structure only, and also directly the proposed mechanism of action can be accounted for in terms of the chemical reactivity of the compounds under study [11]. In several cases the parameters connected with the electronic and the chemical structure of the molecule act concurrently on the inhibitor efficiency and it is difficult to decide which parameter plays the most important role in increasing the inhibitor efficiency [12]. Silva *et al.* [35] reported the bio guided phytochemical studies which allowed the identification of the four flavonoids compounds (Kaempferol, Quercetin, Myricetin, Rhamnetin) of interest from *G. senegalensis* leaves extract. This research work intends to study the performance of the four selected flavonoid compounds of the leaves extract of *Guirea senegalensis* for corrosion inhibition of pure Aluminium Al(1 1 0) metal through computational approaches.

2. Methodology

2.1 Sketching the Inhibitor Molecules and Geometry Optimization

The inhibitor molecules of interest (Kaempferol, Quercetin, Myricetin and Rhamnetin) were sketched using ChemDraw Ultra 7.0 software. The sketched molecules were all subjected to geometry optimization in order to refine the geometry of their structures so as to minimize their conformational and torsional energies. This task was accomplished using the DMol^3 geometry optimization contained in Accelrys Material Studio 7.0 software. The optimized structures were saved for further use in quantum calculations of some electronic and structural properties [13].

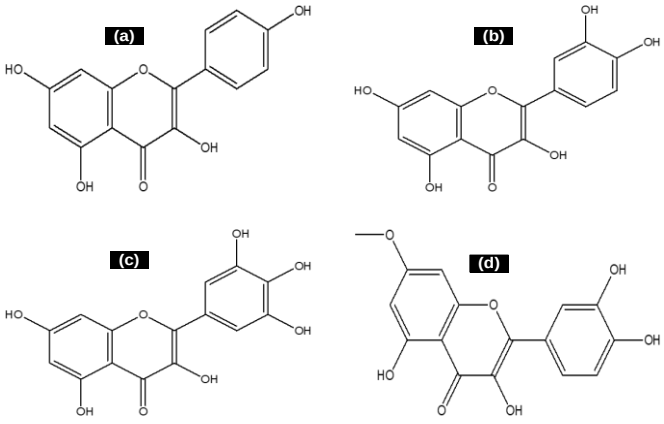

Figure 1. The sketched 2D structures of the four flavonoid molecules under study; (a) Kaempferol (b) Quercetin (c) Myricetin (d) Rhamnetin.

2.2 Quantum Chemical Calculations

All theoretical computations were performed using the density functional theory (DFT) package (DMol^3) with B3YLP: 6-31G functional and DND as the basis set programs as contained in the Materials Studio 7.0 software (Accelrys, Inc.). This provides a very useful tool for understanding molecular properties and for describing the behaviour of atoms in molecules [14, 15]. The calculations provide an insight into chemical reactivity and selectivity, in terms of global reactivity such as electronegativity (χ), global hardness (η), global softness (σ), frontier orbitals (HOMO and LUMO) and local reactivity such as the Fukui function F(r) and local softness S(r) [15-19]. Ionization potential (I) and Electron affinity (A) which are related to the energy of the highest occupied molecular orbital (E_{HOMO}) and lowest unoccupied molecular orbital (E_{LUMO}) and molecular weight of each molecule were all calculated using the following equations [18-22]:

$$\chi = \mu = -(\frac{\partial E}{\partial N})v(r) \quad (1)$$

Where μ is the chemical potential. It is the negative of the electronegativity χ for an N-electron system with total electronic energy E and an external potential v(r). This can also be defined as the first derivative of E with respect to N at constant external potential v(r).

$$\eta = \left(\frac{\partial E^2}{\partial N^2}\right) v(r) = \left(\frac{\partial u}{\partial N}\right) v(r) \quad (2)$$

Where η is called the global hardness, which can be defined within the density functional theory (DFT) as the second derivative of energy E with respect to number of atoms N at constant v(r).

$I = -E_{HOMO}$ (3)

$A = -E_{LUMO}$ (4)

Where I is the ionization potential and A is the electron affinity which are related in terms of energy of the highest occupied molecular orbital (E_{HOMO}) for ionization potential (I) and of the lowest unoccupied molecular orbital (E_{LUMO}) for electron affinity (A).

$$\chi = \frac{(I+A)}{2} = -\frac{E_{LUMO}+E_{HOMO}}{2} \quad (5)$$

$$\eta = \left(\frac{I-A}{2}\right) = -\frac{E_{LUMO}-E_{HOMO}}{2} \quad (6)$$

$$\sigma = 1/\eta \quad (7)$$

Where χ is the electronegativity, η is the global hardness, σ is the Global softness, I is the electron affinity, A is the ionization potential, E_{HOMO} is the energy of the highest occupied molecular orbital and E_{LUMO} the lowest unoccupied molecular orbital.

Fraction of electrons transferred (ΔN) from the inhibitor molecule to the pure aluminium metal surface was calculated using equation (8):

$$\Delta N = \frac{\chi Al - \chi inh}{2(\eta Al - \eta inh)} \quad (8)$$

Where χ_{Al} = 5.6eV and χ_{inh} is the absolute electronegativity of aluminium and the inhibitor molecule respectively. η_{Al} = 0 and η_{inh} stands for absolute global hardness of aluminum and the inhibitor molecule respectively.

The Fukui function f(r) is defined as the first derivative of the electronic density q(r) with respect to the number of electrons N at constant external potential v(r) using a scheme of finite difference approximations from Mullikan population analysis of atoms for all the molecules under study. Calculations for the nucleophilic attack F_K^+ and electrophilic attack F_K^- were performed using equations (9) and (10) respectively as contained in the software.

$F_K^+ = q_K(N+1) - q_k(N)$ (9)

$F_k^- = q_k(N) - q_k(N-1)$ (10)

q_k is the gross charge of atom k in the molecule, which is the electron density at a point r in space around the molecule. N corresponds to the number of electrons in the molecule. N + 1 corresponds to an anion, with an electron added to the LUMO of the neutral molecule, N - 1 corresponds to the cation with an electron removed from the HOMO of the neutral molecule. All calculations were performed at the ground state geometry. These functions were condensed to the nuclei by using an atomic charge partitioning scheme, such as Mullikan and Hirshfeld population analysis.

2.3 Molecular Dynamics Simulation

Molecular Dynamics (MD) simulations were conducted at a molecular level using Forcite quench dynamics in order to sample many different low-energy configurations and to find the low-energy minima for the adsorption of each inhibitor molecule on the Al(1 1 0) metal surface as contained in the Materials Studio 7.0 software (Accelrys, Inc.) [5]. Calculations were performed in a 4 × 3 super cell using the condensed-phase optimized molecular potentials for atomistic simulation studies (COMPASS) force field and the Smart algorithm in the software. Al(1 1 0) is the most densely packed and also the most stable among several types of Al surfaces [22-24]. The Al crystal was cleaved along the (1 1 0) plane. The Al slab built for the docking process was larger than the inhibitor molecules in order to avoid edge effects during docking. Temperature was fixed at 350 K, with NVE ensemble, with time step of 1 fs and simulation time of 5 ps. The system was quenched every 250 steps with the Al(1 1 0) surface atoms constrained. The structures of the inhibitor molecule previously optimized were used for the simulation process. Adsorption of a single inhibitor molecule onto the Al(1 1 0) surface offers access to the adsorption energetics and its effect on the inhibition performance of the molecule [23]. The adsorption energy E_{ads} and the binding energy (BE) between the inhibitor molecule and Al(1 1 0) surface were calculated using equation (10):

$E_{ads} = -BE = E_{Al+Mol} - (E_{Mol} + E_{Al})$ (10)

Where E_{ads} is the adsorption energy equal to negative of binding energy, E_{Al+Mol} is the energy which corresponds to the total energies of Al(1 1 0) surface and the inhibitor molecule, E_{Mol} is the energy of the inhibitor molecule and E_{Al} is the energy of aluminum [23].

3. Results and Discussion

3.1 Quantum Chemical Calculations

To describe the electronic structures, calculations were performed in order to establish the active sites and local reactivity of all the studied molecules. Simulations were performed by means of the DFT electronic structure program DMol^3 using a Mullikan population analysis [25-26]. Electronic parameters for the simulation include unrestricted spin polarization using the DND basis set and the Perdew–Wang (PW) local correlation density functional [5]. The results in Figures 2-5 illustrate (a) the optimized structure, (b) electron density, (c) highest occupied molecular orbital (HOMO) and (d) lowest unoccupied molecular orbital (LUMO) of the studied molecules i.e., Kaempferol, Quercetin, Myricetin and

Rhamnetin respectively. The optimized molecules represent the refined molecules that are brought to a stable geometry with a minimized torsional strength. In Figure 2(b), 3(b), 4(b) and 5(b), the electron cloud is saturated all around the studied inhibitor molecules which facilitate flat-lying adsorption orientations of the inhibitor onto Al(1 1 0) surface. The regions of high HOMO density on the inhibitor molecule are the sites at which electrophiles attack and represent the active centres, with the greatest ability to bond to the Al metal surface, these region of HOMO orbital are saturated on hydroxyl functional group of all the inhibitor molecules as shown in Figure 2(c), 3(c), 4(c) and 5(c), LUMO orbital on the other side, can accept the electrons from the p-orbital of the metal by means of antibonding orbitals to form feedback donations [5, 10].

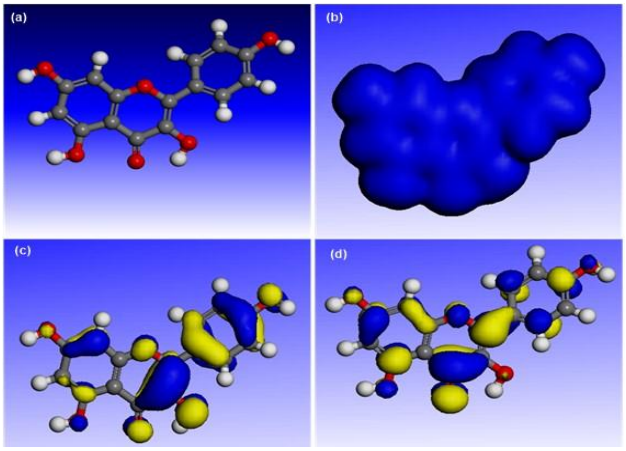

Fig 2. (a) Optimized structure, (b) Electron density around the optimized structure, (c) HOMO of the optimized structure and (d) LUMO of the optimized structure for Kaempferol.

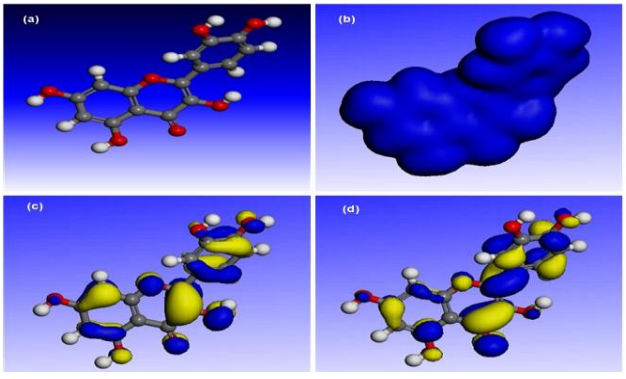

Fig 3. (a) Optimized structure, (b) Electron density around the optimized molecule, (c) HOMO of the optimized of molecule and (d) LUMO of the optimized structure of Quercetin molecule.

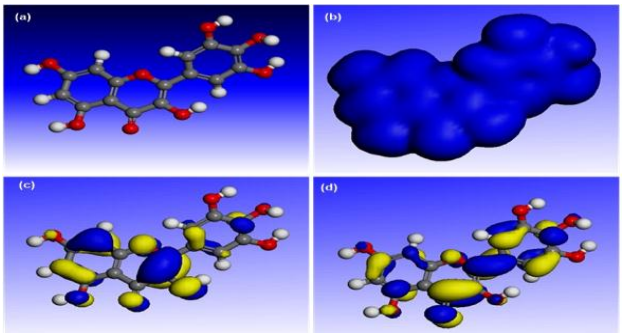

Fig 4. (a) Optimized molecule, (b) Electron density around the optimized molecule, (c) HOMO of the optimized molecule and (d) LUMO of the optimized Myricetin molecule.

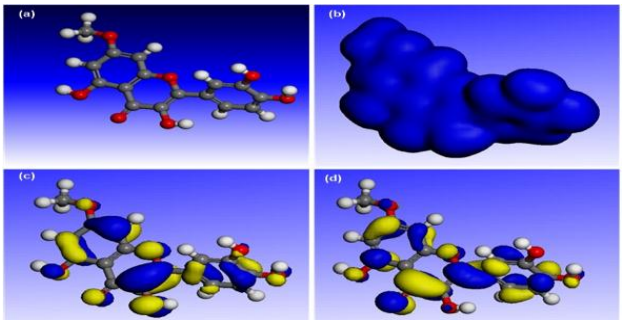

Fig 5. (a) Optimized molecule, (b) Electron density around the optimized molecule, (c) HOMO for the optimized molecule and (d) LUMO for the optimized Rhamnetin molecule.

The result presented in Table 1, shows the eigenvalues of the highest occupied molecular orbital (E_{HOMO}), lowest unoccupied molecular orbital (E_{LUMO}), energy gap and other quantum chemical parameters. The highest E_{HOMO} (-5.766) was obtained in Kaempferol molecule while least in E_{HOMO} (-5.970) was obtained in Myricetin molecule. High value of E_{HOMO} decreased the value of ΔE and high value of E_{LUMO} increased the value of ΔE, the smaller the energy gap between the HOMO and LUMO energy which is a function of reactivity, the stronger interaction of inhibitor molecule with the metal surface [28]. High values of E_{HOMO} indicate the disposition of the molecule to donate electrons to an appropriate acceptor like the unoccupied molecular orbital of the Al metal. Thus, a ΔE low value shows good inhibition efficiencies of the organic inhibitor because the energy to remove an electron from the last occupied orbital will be minimized [29-30].

The values of E_{HOMO} obtained show no significant difference between all the molecules which is due to the similarity of their molecular size containing the HOMO. The similarities in quantum chemical parameters mean that the adsorption strengths of the molecules will be mostly determined by molecular size parameters rather than

electronic structure parameters [5, 21]. Also, excellent organic inhibitors not only donate electrons to a vacant orbital of the metal, but they also accept free electrons from the metal which makes them more electron rich and therefore offer better inhibition efficiency. The result obtained in Table 1 shows that all the inhibitor molecules are rich in electrons since higher value of E_{LUMO} is an index that indicate the tendency of a molecular specie to accept free electrons and offer good inhibition performance. The values of the fraction of electron transferred from inhibitor molecule to the metal surface (ΔN) ranges from (0.412-0.772) with Myricetin having the lowest value 0.412 and Kaempferol having the highest value of 0.772 (Table 1). All these values are all less than 3.6 which indicate that inhibition efficiency increases with increase in values of the electron donating ability of the molecules while ΔN greater than 3.6 indicates that inhibition efficiency decreases with increasing values of the electron donating ability of the molecules [5]. The difference in electronegativity between the molecules and aluminium drives the electron transfer. Therefore, all the studied molecules inhibit the corrosion of Al and has the performance in the following order Kaempferol < Rhamnetin < Quercetin < Myricetin with Myricetin having the lowest ΔN value (0.412) shows relatively better inhibition efficiency amongst others [31].

Table 1: Quantum chemical parameters for all the studied inhibitor molecules

Parameters	KFR	QCT	MRT	RMT
HOMO (at orbital number)	74	78	82	82
LUMO (at Orbital number)	75	79	83	83
E_{HOMO} (eV)	-5.77	-5.87	-5.97	-5.84
E_{LUMO} (eV)	-1.77	-1.65	-1.68	-1.55
Energy gap (ΔE) (eV)	4.00	4.21	4.29	4.32
Molecular weight ($gmol^{-1}$)	286	302	318	316
Ionization potential (I) (eV)	5.77	5.87	5.97	5.84
Electron Affinity (A) (eV)	1.77	1.65	1.68	1.54
Global hardness (η)	2.00	2.11	2.15	2.15
Global softness (σ)	0.50	0.47	0.47	0.47
Absolute Electronegativity (χ)	2.51	3.76	3.83	3.69
Fraction of Electron Transfer ΔN	0.77	0.44	0.41	0.44

KFR: Kaempferol, QCT: Quercetin, MRT: Myricetin, RMT: Rhamnetin

Table 2 gives the Fukui indices values for Electrophilic (F^-) and Nucleophilic (F^+) attack by Mullikan and Hirshfield model for all the studied molecules. While Figure 6 below is the 3D structures for all the molecules corresponding to the highest Fukui values for specific atom in Table 2. This result shows the local reactivity of each molecule by means of Fukui indices which indicates the regions of electrophilic and nucleophilic attack for all the molecules. F^- measures reactivity with respect to electrophilic attack or the ability of the molecule to release electrons, whereas F^+ measures reactivity relating to nucleophilic attack or tendency of the molecule to attack electrons. Based on the results obtained in Table 2 for the electrophilic attack, Kaempferol, Quercetin, Myricetin and Rhamnetin has both their highest Mullikan and Hirshfeld charges on (O)3, (O)3, (O)3 and (O)15 respectively, while for the nucleophilic attack, both their Mullikan and Hirshfeld charges are on (O)5, (O)5, (O)5 and (O)11. The first three molecules all have their electrophilic attack on (O)3 oxygen of hydroxyl group (-OH) and nucleophilic attack on (O)5 of ketone functional group (O=C-), this could be attributed to similarities in their chemical structure with identical –OH and ketone functional groups that comprised of HOMO and LUMO orbital respectively. The region of a molecule where the Fukui function is large are chemically softer than the region where the Fukui function is small, and by invoking the hard and soft acid and base (HSAB) principle in a local sense, one may establish the behaviour of the different sites with respect to hard or soft reagents [20-21]. Thus, all the molecules can accept electrons and also release electrons mostly through the active centres specified by the Mullikan and Hirsheld model as one can clearly see those centres on HOMO and the LUMO orbital in Figure 2(c), 3(c) 4(c) and 5(c) and figure 2(d), 3(d) 4(d) and 5(d) respectively. Interestingly, those active sites for donor and acceptor of electrons are clearly shown in Figure 6, where by each atom is specified by a unique number.

Table 2: Fukui Functions for all the Inhibitor molecules

Molecules	**Electrophilic (F^-)**		**Nucleophilic (F^+)**	
	Mullikan	Hirshfeld	Mullikan	Hirshfeld
Kaempferol	(O3) 0.094	(O3) 0.089	(O5) 0.106	(O5) 0.106
Quercetin	(O3) 0.096	(O3) 0.090	(O5) 0.109	(O5) 0.106
Myricetin	(O3) 0.100	(O3) 0.095	(O5) 0.106	(O5) 0.103
Rhamnetin	(O15) 0.100	(O15) 0.093	(O11) 0.110	(O11) 0.107

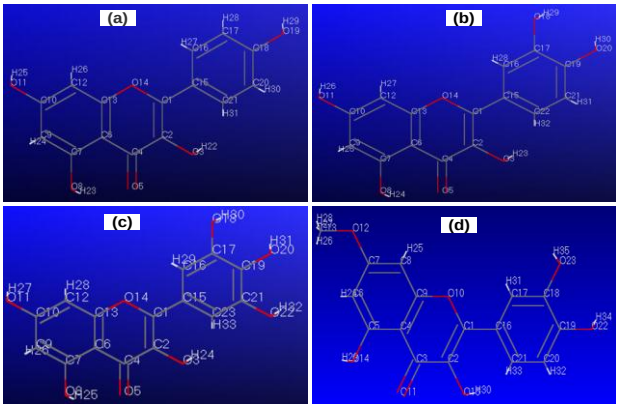

Figure 6. The 3D labelled structures for (a) Kaempferol, (b) Quercetin, (c) Myricetin and (d) Rhamnetin molecules.

3.2. Molecular Dynamic Simulations

Molecular Dynamics (MD) was carried out at molecular level by MD simulations using Forcite quench dynamics to sample many different low-energy configurations in order to identify the low-energy minima for the adsorption of the each studied molecule on the metal surface. The total energies were calculated by averaging the energies of the five most stable representative adsorption configuration of each molecule. The side view snapshot for the lowest energy adsorption configurations for single molecules of Kaempferol, Quercetin, Myricetin and Rhamnetin for the interaction of Al(1 1 0) surface were shown in Figures 7 (a), (b), (c) and (d) respectively. The results indicate that each inhibitor molecule maintained flat-lying adsorption orientation on the Al(1 1 0) surface, as can be seen from the delocalization of the electron density all around the molecules in Figure 2(b), 3(b), 4(b) and 5(b) above. This adsorption configuration maximizes contact between the molecule and the metal surface. The results of adsorption energies for the interaction of each molecule with the Al (1 1 0) surface via Forcite Quench Dynamics were presented in Table 3. It has been reported that, the more negative the E_{ads} (or more positive the BE) of the inhibitor-metal surface interaction is, the better the adsorption or the higher the binding of the inhibitor onto the metal surface and subsequently the higher the inhibition efficiency of the molecule [32-33]. Based on the E_{ads} or BE values obtained, Myricetin having more negative value of E_{ads}(-84.213±0.621Kcalmol^{-1}) or more positive value for BE (84.213±0.621Kcalmol^{-1}) is expected to perform better in inhibiting the corrosion of aluminum. This could be related to the order of molecular size, with larger molecules more strongly adsorbed on the metal surface. It can be observed that the magnitude of calculated E_{ads} or BE values are all less than 100kcalmol^{-1}, despite the fact that the simulations did not put into consideration the specific covalent interactions between the molecules and the aluminum surface. Values less than or equal to 100kcalmol^{-1} have been reported to be in the range of physical interactions [21, 32]. Therefore, adsorptions of these molecules on Al surface in terms of their binding energy increases in the following order; Kaempferol < Rhamnetin < Quercetin < Myricetin. This observation can be attributed to their molecular size, and the entire molecule adsorbed with a flat orientation on the Al(1 1 0) surface [34].

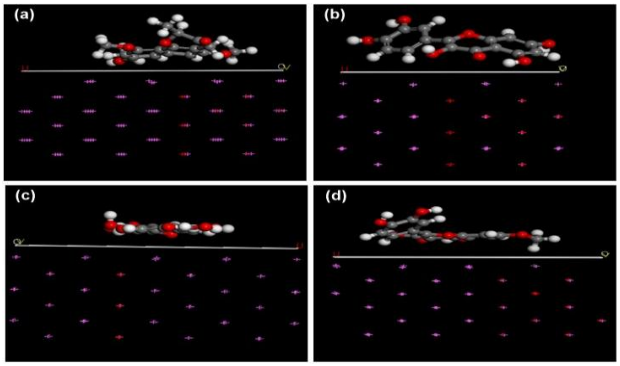

Fig 7. The side view snap shots for the adsorption of (a) Kaempferol, (b) Quercetin (c) Myricetin and (d) Rhamnetin molecule on the Al(110) metal surface.

Table 3: Calculated Adsorption Parameters for the Interaction of the Studied Molecules with the Al(1 1 0) Surface via Forcite Quench Dynamics.

Molecule	Total Potential Energy (kcal/mol)	Molecular Energy (kcal/mol)	Energy of Al(110) surface (kcal/mol)	Adsorption Energy (kcal/mol)	Binding Energy (kcal/mol)
Kaempferol	-126.609 ±3.531	-48.009 ±6.235	0.000 ±000	-78.600 ±1.327	78.600 ±1.327
Quercetin	-142.989 ±4.224	-60.333 ±3.301	0.000 ±000	-82.656 ±4.517	82.656 ±4.517
Myricetin	-171.128 ±2.315	-86.915 ±3.121	0.000 ±000	-84.213 ±0.621	84.213 ±0.621
Rhamnetin	-141.245 ±2.342	-61.324 ±5.615	0.000 ±000	-79.921 ±2.579	79.921 ±2.579

4. Conclusions

This work revealed that molecules of flavonoids compound from *Guiera Senegalensis* leaves can inhibit the corrosion of aluminum metal. Quantum chemical parameters associated with the electronic structures of the inhibitor molecules confirmed their inhibiting potential through HOMO, LUMO, ΔN, electron density, while Fukui indices indicates that the molecules may adsorb to the Al metal surface trough the hydroxyl (–OH) and carbonyl (-C=O)

functional groups. The molecular dynamics simulation results showed that all inhibitors have some adsorption energies less than 100kcalmol^{-1} and could adsorb on the aluminum metal surface in the same pattern showing a great similarity in the structure of these four selected compounds. The adsorption energy of these compounds was found to have a direct relation with their molecular weight, the adsorption energy increases with increase in molecular weight of the inhibitor molecule which in turn increases the inhibition efficiency.

Acknowledgements

The authors wish to appreciate the contribution of Dr. David Arthur of the Baze University, Abuja, Nigeria for the initial installation of the Accelrys Materials Studio 8.0 software programme.

Conflict of Interest

The authors declare that they have no conflict of interest

References

1. Sethi T, Chaturvedi A, Upadhyaya RK, Mathur SP. Synergistic inhibition between Schiff's bases and sulfate ion on corrosion of aluminium in sulfuric acid. *Protection of Metals and Physical Chemistry of Surfaces*. 2009;45(4):466-71.
2. Rani BE, Basu BB. Green inhibitors for corrosion protection of metals and alloys: an overview. International Journal of corrosion. 2012. https://doi.org/10.1155/2012/908290
3. El-Haddad MN. Chitosan as a green inhibitor for copper corrosion in acidic medium. *International Journal of Biological Macromolecules*, 2013,55: 142-149.
4. Ladha DG, Wadhwani PM, Lone MY, Jha PC, Shah NK. Evaluation of Fennel Seed Extract as a Green Corrosion Inhibitor for Pure Aluminum in Hydrochloric Acid: An Experimental and Computational Approach. *Anal. Bioanal. Electrochem*. 2015;7:59-74.
5. Ayuba AM, Uzairu A., Abba H, Shallangwa GA. Hydroxycarboxylic acids as corrosion inhibitors on aluminium metal: a computational study. *Journal of Materials and Environmental Sciences*, 2018a; 9;11: 3026-3034.
6. Abd El Rehim SS, Hassan HH, & Amin, MA. The corrosion inhibition study of sodium dodecyl benzene sulphonate to aluminium and its alloys in 1.0 M HCl solution. *Materials Chemistry and Physics*, 2002; 78: 337-348.
7. Bensajjay F, Alehyen S, El Achouri M, & Kertit S. Corrosion inhibition of steel by 1-phenyl 5-mercapto 1, 2, 3, 4-tetrazole in acidic environments (0.5 M H_2SO_4 and 0.3 M H_3PO_4). *Anti-Corrosion Methods and Materials*. 2003;.50; 6: 402-409.
8. Oguzie EE. Corrosion inhibition of aluminium in acidic and alkaline media by Sansevieria trifasciata extract. *Corrosion Science*, 2007;49;3: 1527-1539.
9. Rodríguez-Valdez LM, Martínez-Villafañe A, & Glossman-Mitnik D. CHIH-DFT theoretical study of isomeric thiatriazoles and their potential activity as corrosion inhibitors. *Journal of Molecular Structure: THEOCHEM*, 2005; 716(1-3), 61-65.
10. Ebenso EE, Isabirye DA, & Eddy NO. Adsorption and Quantum Chemical Studies on the Inhibition Potentials of Some Thiosemicarbazides for the Corrosion of Mild Steel in Acidic Medium. *International Journal of Molecular Sciences*, 2010;*11*, 2473-2498.
11. Gece G. The use of quantum chemical methods in corrosion inhibitor studies. *Corrosion Science*, 2008; 50: 2989-2992.
12. Khaled K, & Al-Qahtani M. The inhibitive effect of some tetrazole derivatives towards Al corrosion in acid solution: chemical, electrochemical and theoretical studies. *Materials Chemistry and Physics*, 2009; 113;1; 150-158.
13. Eddy NO, Ibok UJ, Ebenso EE, El Nemr A, & El Sayed H. Quantum chemical study of the inhibition of the corrosion of mild steel in H_2SO_4 by some antibiotics. *Journal of molecular modeling*, 2009; 15;9: 1085-1092.
14. Obot I, Obi-Egbedi N, Ebenso E, Afolabi A, & Oguzie E. Experimental, quantum chemical calculations, and molecular dynamic simulations insight into the corrosion inhibition properties of 2-(6-methylpyridin-2-yl) oxazolo [5, 4-f][1, 10] phenanthroline on mild steel. *Research on chemical intermediates*, 2013; 9;5: 1927-1948.
15. Obi-Egbedi NO. and Ojo ND. Computational studies of the corrosion inhibition potentials of some derivatives of 1H-Imidazo [4, 5-F] [1, 10] phenanthroline, *Journal of Science Research*, 2015; 14: 50-56.
16. El-Maksoud SA. Studies on the effect of pyranocoumarin derivatives on the corrosion of iron in 0.5 M HCl. *Corrosion Science*, 2002; 44;4: 803-813.
17. Kumar A., Shukla R., & Venkatachalam A. Studies of corrosion and electrochemical behavior of some metals and brass alloy under different media. *Rasayan J. Chem*, 2013; 6;1: 12-14.
18. Eddy NO, Ameh PO, & Essien NB. Experimental and computational chemistry studies on the inhibition of aluminium and mild steel in 0.1 M HCl by 3-nitrobenzoic acid. *Journal of Taibah University for Science*, 2018; 12; 5; 545-556.

19. Salman TA, Al-Azawi KF, Mohammed IM, Al-Baghdadi SB, Al-Amiery AA, Gaaz TS, Kadhum AA. *Results in Physics*, 2018*;* 10:291-296.
20. Sundari C, Setiadji S, Ramdhani MA, Ivansyah A, & Widhiasari N. Additional Halogen Group (F, Cl, and Br) to 2-Phenyl-imidazole [1, 2α] pyridine on Corrosion Inhibition Properties: A Computational Study. *Mater. Sci. Eng*, 2018; 288, 012033.
21. Ayuba AM, Uzairu A, Abba H, & Shallangwa GA. Theoretical study of aspartic and glutamic acids as corrosion inhibitors on aluminium metal surface. *Moroccan Journal of Chemistry*, 2018b; *6;* 1: 2160-2172.
22. Lgaz H, Salghi R, Chaouiki A, Jodeh S, Bhat KS. Pyrazoline derivatives as possible corrosion inhibitors for mild steel in acidic media: A combined experimental and theoretical approach. *Cogent Engineering*. 2018 Jan 1;5(1):1441585.
23. Zhao H, Zhang X, Ji L, Hu H, Li Q. Quantitative structure-activity relationship model for amino acids as corrosion inhibitors based on the support vector machine and molecular design. *Corrosion Science*, 2014; 83:261-271.
24. Mishra A, Verma C, Srivastava V, Lgaz H, Quraishi MA, Ebenso EE, Chung M. Chemical, electrochemical and computational studies of newly synthesized novel and environmental friendly heterocyclic compounds as corrosion inhibitors for mild steel in acidic medium. *Journal of Bio- and Tribo-Corrosion*, 2018; 4:32.
25. Delley B. An all-electron numerical method for solving the local density functional for polyatomic molecules. *The Journal of Chemical Physics*, 1990; 92*;*1: 508-517.
26. Delley B. From molecules to solids with the DMol 3 approach. *The Journal of Chemical Physics*, 2000; 113;18: 7756-7764.
27. Khaled K. Corrosion control of copper in nitric acid solutions using some amino acids–a combined experimental and theoretical study. *Corrosion Science*, 2010; 52;10: 3225-3234.
28. Xia S, Qiu M, Yu L, Liu F, & Zhao H. Molecular dynamics and density functional theory study on relationship between structure of imidazoline derivatives and inhibition performance. *Corrosion Science*, 2008; 50;7: 2021-2029.
29. Yurt A, Ulutas S, & Dal H. Electrochemical and theoretical investigation on the corrosion of aluminium in acidic solution containing some Schiff bases. *Applied Surface Science*, 2006; 253; 2: 919-925.
30. Obot IB, Ebenso EE, & Kabanda MM. Metronidazole as environmentally safe corrosion inhibitor for mild steel in 0.5 M HCl: experimental and theoretical investigation. *Journal of Environmental Chemical Engineering*, 2013; 1; 3: 431-439.
31. Khaled K, & Amin MA. Computational and electrochemical investigation for corrosion inhibition of nickel in molar nitric acid by piperidines. *Journal of Applied Electrochemistry*, 2008; 38; 11: 1609-1621.
32. John S, & Joseph A. Quantum chemical and electrochemical studies on the corrosion inhibition of aluminium in 1N HNO_3 using 1, 2, 4-triazine. *Materials and Corrosion*, 2013; 64;7: 625-632.
33. Awe FE, Idris SO, Abdulwahab M, & Oguzie EE. Theoretical and experimental inhibitive properties of mild steel in HCl by ethanolic extract of *Boscia senegalensis*. *Cogent Chemistry*. 2015. http://dx.doi.org/10.1080/23312009.2015.1112676
34. Li X, Deng S, & Xie X. Experimental and theoretical study on corrosion inhibition of o-phenanthroline for in HCl solution. *Journal of the Taiwan Institute of Chemical Engineers*, 2014; 45*;*4: 1865-1875.
35. Silva O, Serrano R, Gomes ET. Botanical characterization of *Guiera senegalensis* leaves. *Microscopy and Microanalysis*, 2008; 14;5: 398-404.

Recommended Citation

Ayuba A M, Abubakar M. DFT and molecular dynamic simulation study on the corrosion inhibition of Aluminum by some flavonoids of *Guiera Senegalensis* leaves. *Alg. J. Eng. Tech. 2021*, 4:66-73. http://dx.doi.org/10.5281/zenodo.4636546